8-6-2013

In Situ Study of the Photodegradation of Carbofuran Deposited on TiO_2 Film under UV Light, Using ATR-FTIR Coupled to HS-MCR-ALS

Abderrahman Atifi
Marquette University

Kazimierz Czarnecki
Marquette University

Hafida Mountacer
Universite Hassan Ier - Settat

Michael D. Ryan
Marquette University, michael.ryan@marquette.edu

Accepted version. *Environmental Science & Technology*, Vol 47, No. 15 (August 6, 2013): 8650-8657. DOI.

In Situ Study of the Photodegradation of Carbofuran Deposited on TiO_2 Film under UV Light, Using ATR-FTIR Coupled to HS-MCR-ALS

Abderrahman Atifi
Chemistry Department, Marquette University, Milwaukee, WI
Laboratoire des Sciences de l'Environnement et du Developement, Equipe de Chimie Ecologique, FST, Universite Hassan 1er, Settat 26000, Morocco
Kazimierz Czarnecki
Chemistry Department, Marquette University, Milwaukee, WI
Hafida Mountacer
Laboratoire des Sciences de l'Environnement et du Developement, Equipe de Chimie Ecologique, FST, Universite Hassan 1er, Settat 26000, Morocco
Michael D. Ryan
Chemistry Department, Marquette University, Milwaukee, WI

Environmental Science & Technology, Vol 47, No. 15 (August 6, 2013): pg. 8650-8657. DOI.

Abstract

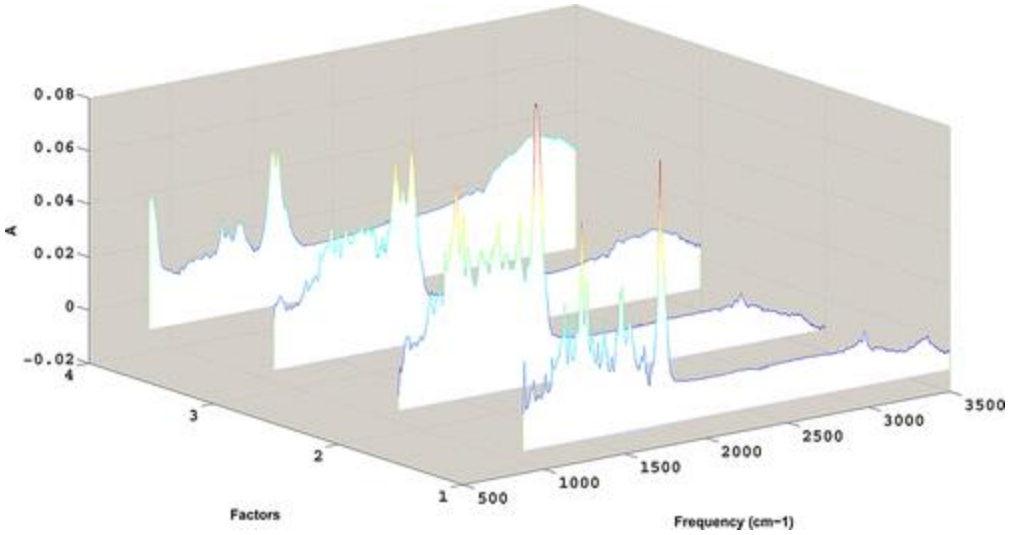

The in situ study of the photodegradation of carbofuran deposited on a TiO_2 catalyst film under UV light was carried out using the ATR-FTIR technique. The data were analyzed using a Hard–Soft Multivariate Curve Resolution-Alternating Least Squares (HS-MCR-ALS) methodology. Using S-MCR-ALS, four factors were deduced from the evolving factor analysis of the data, and their concentrations and spectra were determined. These results were used to draw qualitative and quantitative analyses of the major products of carbofuran photodegradation. The results of this analysis were in good agreement with GC-MS results and with reported mechanisms. Hard-MCR-ALS was then used to refine the spectra and concentrations, using a multistep kinetic model. The rate constant for the first step in the photodegradation of carbofuran was found to be 2.9×10^{-3} min^{-1}. The higher magnitude of the correlation (96.87%), the explained variance (99.87%) and LOF (3.01), are good indicators of the reliability of the outcome of this approach. This method has been shown to be an efficient approach to study in situ photodegradation of pesticides on a solid surface.

Introduction

Carbofuran (2,3-dihydro-2,2-dimethyl-7-(N-methylcarbamate-7-benzofuranol) is a broad-spectrum carbamate insecticide and nematicide widely used to control several soil-borne insects and nematodes found in potatoes, corn, rice, alfalfa, grapes, and other agricultural crops. It is an inhibitor of acetyl-cholinesterase and highly toxic to fish and mammals.[1,2] This pesticide is directly sprayed onto soil and plants immediately after emergence, presenting itself as a potential pollutant. Therefore, a study of its photolysis in solid phase,

Environmental Science & Technology, Vol 47, No. 15 (August 6, 2013): pg. 8650-8657. DOI.

as one important pathway of its degradation, is needed. However, studying photodegradation on solid surfaces is more difficult than in solution and suspension for several reasons. First, there is the difficulty in the quantification of light absorption in thicker particulate layers. Second, extraction of adsorbed photoproduct could prevent the detection of labile products. Third, it is difficult to maintain homogeneous conditions (temperature, humidity, composition) in thicker layers of particles.[3,4]

A suitable approach to avoid these difficulties consists of irradiation of micrometer thick layers of particles coated on an attenuated total reflectance (ATR) element while monitoring the phototransformation by infrared spectroscopy. ATR-FTIR has been applied previously to study adsorption of organic molecules on oxide layers.[5-8] Using this technique allows for monitoring the disappearance of the initial compound and the appearance of a range of functional groups, while obtaining real time information on the system without disturbing the system.

Although infrared spectroscopy has been employed for qualitative and quantitative analysis, the identification of each component from FTIR mixture spectra is difficult, particularly when photoproducts have very similar structures with widely overlapped absorption bands. While it is easier to obtain quality spectra when the concentration of the substrate is large, the amount of photochemical product may not be sufficient to be observed in the presence of the starting substrate. On the other hand, low concentrations of substrate make it difficult to obtain high quality spectra. One way to overcome this limitation is by using a catalyst film, with higher substrate concentrations, so that one can observe detectable kinetics. For instance, Araña et al. have recorded FTIR measurements to follow the degradation of highly concentrated phenolic solutions by TiO_2 photocatalysis and photo-Fenton process.[9,10] The photocatalytic properties of semiconducting TiO_2 particles have been extensively studied as a promising method for the treatment of organic contaminants.[11-13] In the presence of oxygen, illumination of TiO_2 particles produces hydroxyl radicals, known as potential oxidants of organic molecules.

Environmental Science & Technology, Vol 47, No. 15 (August 6, 2013): pg. 8650-8657. DOI.

Pesticides can be degraded in the environment by a number of processes. Most closely related to this work would be the degradation of pesticides on dry soil. The focus of this study is on the reaction at solid surfaces. The method described here is an efficient method for identifying the degradation steps in the photolysis of pesticides with a minimum of chemical separation steps. The in situ FTIR method is a rapid and efficient method to identify intermediates for the study of the photolysis of pesticides. This technique eliminates the solvent extraction steps and provides a "greener" procedure for this analysis. In addition to the photodecomposition on solids, an understanding of the kinetics of the reaction would be useful for the development of techniques for the solar photodegradation of pesticides in water.[14] Solid surfaces have been shown to be efficient in the photochemical decomposition of pesticides in water[14-16] and have been proposed as a method for the removal of pesticides from leaching water.[14,16]

ATR-IR spectroscopy has been shown to be an efficient method for the study of photochemical reactions. This methodology has been reviewed by McQuillan[17] to probe the photocatalysis of particle films. Some recent examples of the use of this methodology will be cited here. Mul et al. have used ATR-IR spectroscopy to the study the kinetics of the photochemical oxidation of cyclohexane on solid surfaces.[18-20] This methodology was also utilized by Bürgi et al. to examine the photochemical decomposition of malonic acid.[21,22] Frei et al. have used the rapid scan technique to identify surface intermediates in the oxidations of water.[23]

The combination of infrared spectroscopy with mathematical resolution complements the chemical separation techniques. Having the advantage of exploiting full spectral data points by using simultaneously a large number of analytical signals, Multivariate Curve Resolution Alternating Least Squares (MCR-ALS) has been proposed for the extraction of analytical information from spectroscopic data.[24,25] In this method, data analysis can be achieved by a soft-modeling method (by applying natural constraints) or by a hard-modeling method (when a chemical model is available). Recently, attention has been directed toward the combination of hard- and soft-modeling methods to have the advantages of both methods and to obtain more reliable results.[26,27]

Environmental Science & Technology, Vol 47, No. 15 (August 6, 2013): pg. 8650-8657. DOI.

The present investigation presents an in situ study of photodegradation of carbofuran deposited on TiO_2 film under UV light, using the ATR-FTIR technique coupled to MCR-ALS methods. The use of HS-MCR-ALS allows examining both kinetic and mechanistic aspects of the photochemical reaction.

Materials and Methods

Experimental Procedure

The catalyst film was first deposited on the surface (3.75 cm^2) of the ATR crystal by applying 0.5 mL of a suspension (6 mg/mL) of TiO_2 (Aeroxide P25 Titania, Aldrich) in methanol (Spectrophotomeric grade, Alfa Aesar) and allowing the solvent to evaporate. Then, 0.5 mL of carbofuran (98%, Aldrich) solution (2 mg/mL) in methanol was pipetted on the TiO_2 film surface and was kept in the dark to dry under ambient air. The overall thickness was 4.2 μm, as a sum of the two layers of 1.9 μm of TiO_2 and 2.3 μm of carbofuran. Spectral measurements started simultaneously with the irradiation, after complete removal of the solvent. There was no infrared spectral evidence for the presence of water in the solid under these conditions. For extraction of the residual pesticide, the film was washed with 20 mL of dichloromethane, filtered with 50 μm filter paper, and analyzed by GC-MS. The TiO_2 was dried under a vacuum overnight prior to use. The experiment was carried out under ambient conditions.

Apparatus

Spectra were recorded on an FTIR spectrophotometer (Spectrum100 Series) equipped with 45° Horizontal ZnSe attenuated total reflectance (ATR) accessory (PIKE MIRacleTM, PIKE technology). The absorbance spectra were the average of 32 spectra at 1 cm^{-1} resolution and over a spectral detection range of 3500–850 cm^{-1} and were taken every 10 min for a total irradiation time of 85 h. A background on TiO_2 film (in the same resolution and scanning conditions) was carried out before depositing the pesticide layer.

Environmental Science & Technology, Vol 47, No. 15 (August 6, 2013): pg. 8650-8657. DOI.

UV light (220–366 nm) was produced by a mercury lamp (Photochem lamp, 5" A.L. UV Immer type), which was placed vertically on top of the ATR accessory, such that the film deposited on the crystal can be spectrally monitored while irradiated. The irradiation chamber was covered with aluminum foil in order to prevent UV light from escaping from the apparatus. The inner temperature was measured at 28 °C during irradiation time. Measured irradiance, in the same conditions and at a distance of 10 cm from the lamp, was I_0 = 5.2 W·cm^{-2}. The temperature of the surface was checked during and at the end of the irradiation time, and no evidence of heating was found.

Chromatographic analysis was carried out by a spectrometer GC-FID (Agilent 6850), equipped with a column HP-5 (5% phenylmethylpolysiloxane, 30 m, 0.32 mm, 0.25 μm). The temperature program of the GC-FID was selected as follows: 80 °C held for 10 min, 80–250 °C at 5 °C min–1, 250 °C held for 60 min. Each sample with 3 μL was injected twice.

Quantum Computations

Full geometry optimizations of carbofuran were carried out by the B3LYP method with the 6-311++G(d,p) basis set used in our previous work.[28] Vibrational frequency analysis was employed to assess the nature of optimized structures. All computations were performed using the Gaussian 09 program.[29]

Chemometric

All ATR-FTIR spectra recorded during the irradiation of carbofuran were arranged in a data matrix $D(r \times c)$ where r(2651) is the number of wavenumbers and c(511) is the number of spectra.

The rank analysis was carried out using singular value decomposition (SVD), and the number of factors (n) was determined by evaluating the real error (RE) and the indicator factor function (IND).[30]

Environmental Science & Technology, Vol 47, No. 15 (August 6, 2013): pg. 8650-8657. DOI.

$$\mathrm{RE} = \left[\sum_{j=n+1}^{c} \frac{\lambda_j^{\circ}}{r(c-n)}\right]^{1/2}; \quad \mathrm{IND} = \frac{\mathrm{RE}}{(c-n)^2}$$

The real error is the difference between the pure error-free data and the raw experimental data,[31] λ_i° are the eigenvalue values from the factor analysis, r and c are the number of rows and columns, respectively, of the data, and n is the number of principal factors. The indicator factor function reaches a minimum when the number of factors (n) in the chemometric analysis is equal to the number of factors in the data.

Evolving factor analysis (EFA) was applied to obtain knowledge about the evolution of the process components throughout the photodegradation reaction, i.e., when they emerge and when they decay.[32] The properly treated EFA results were afterward employed as an initial estimate of the concentration profiles in the first MCR-ALS analysis.[33,34] In this first soft-modeling analysis, unimodality, non-negativity, and closure constraints were applied for concentrations profiles. The resolution quality was evaluated by the explained variance R^2 and the lack of fit (LOF)

$$R^2 = 100 \times \frac{\sum_i \sum_j \hat{d}_{i,j}^{\,2}}{\sum_i \sum_j d_{i,j}^2}; \quad \mathrm{LOF} = 100 \times \sqrt{\frac{\sum_i \sum_j (d_{i,j} - \hat{d}_{i,j})^2}{\sum_i \sum_j \hat{d}_{i,j}^{\,2}}}$$

where d_{ij} is the experimental absorbance at the j^{th} wavenumber in the i^{th} spectrum, and $\hat{d}_{ij}$ is the corresponding value calculated by ALS.

In the HS-MCR-ALS approach, the hard-modeling constraint was applied by fitting the soft-modeled concentrations to a selected kinetic model using the Marquardt–Levenberg algorithm for iterative least-squares fitting of nonlinear parameters.[35] Then the fitted profiles were used to update the soft-modeled ones in the ALS loop, and the rate constants were generated as additional information (Figure 1). The calculations were performed in a MATLAB environment (Mathworks, R2011b).

Environmental Science & Technology, Vol 47, No. 15 (August 6, 2013): pg. 8650-8657. DOI.

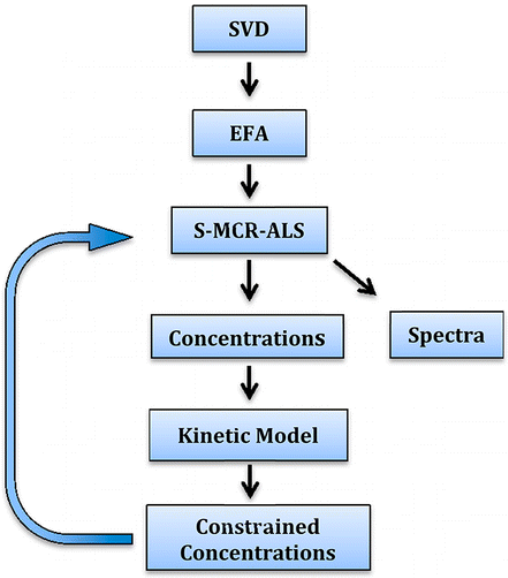

Figure 1. HS-MCR-ALS approach.

Results and Discussion

The photodegradation of carbofuran deposited on TiO_2 film was conducted under UV irradiation, using ATR-FTIR spectroscopy. In order to overcome the sensitivity limitation of this technique, an optimized concentration of 1.0 mg pesticide/3.0 mg substrate was used to enable better spectrum quality, while allowing for a significant phototransformation to occur under our experimental conditions. It is worth noting that an irradiation of deposited carbofuran film alone (without catalyst film) on the ATR crystal, and under the same experimental conditions, did not result in any detectable phototransformation (no changes in the spectrum).

Band Assignments

Vibrational spectral assignments have been performed on the recorded ATR-FTIR spectrum based on the theoretically predicted wavenumbers by the B3LYP method using the 6-311++G(d,p) basis set. The observed spectra are in good agreement with the simulated spectra shown in Table 1. Six major peaks were identified 3360, 2975, 1715, 1617, 1233, and 1127 cm^{-1} corresponding respectively to N–H, C–H, C═O, C═C, C–O, and C–N bonds. Atomic displacements of selected modes are shown in the Supporting Information.

Environmental Science & Technology, Vol 47, No. 15 (August 6, 2013): pg. 8650-8657. DOI.

Table 1. Bands Assignment and Their Vibrational Modes Using DFT Calculations

experimental		B3LYP/6-311++G(d,p)		
frequency (cm^{-1})	**absorbance**	**frequency[a] (cm^{-1})**	**intensity**	**vibrational mode**
3360	0.16	3643.6	101.00	N–H Str
2975	0.05	3106.1	52.73	C–H Str
1715	0.6	1744.7	758.85	C═O Str
1617	0.03	1644.9	24.42	C═C Ar Str
1233	0.3	1236.5	381.55	C–O Str
1127	0.21	1124.6	154.70	C–N Str

[a]Nonscaled frequencies. To our knowledge, no scaling factor was reported for B3LYP/-6311++G(d,p). A linear correlation (R^2 = 99.52%) between calculated and experimental frequencies is included in the Supporting Information.

Exploratory Analysis

The ATR–FTIR spectra recorded during the photodegradation of carbofuran under UV light is shown in Figure 2. A preliminary examination of the spectral evolution during the irradiation time showed the important changes in the different spectral zones. During the first few hours, the intensities of N–H and C–N peaks decreased, while a new band appeared at 1650 cm^{-1}. As the exposure time increased, another new band appeared at 3400 cm^{-1}, while the C–O and C═O bands decreased. In fact, the interpretation of these variations was complex and needed to be deconvoluted using chemometric methods.

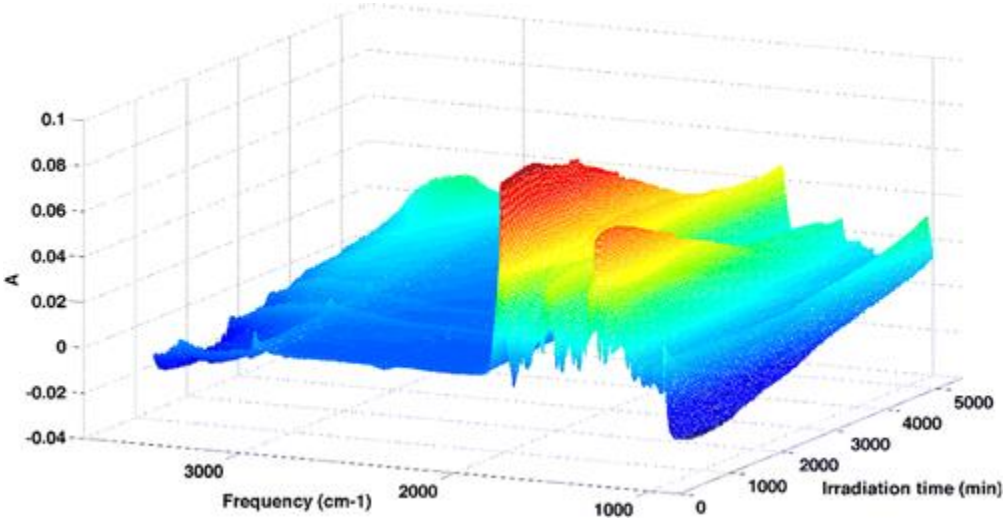

Figure 2. Evolution of ATR-FTIR spectrum of deposited carbofuran on the TiO_2 film as a function of irradiation time.

Chemometric Analysis

In order to understand the spectral changes, we considered the HS-MCR-ALS approach introduced above. The first step was the determination of the number of principal factors by subjecting our experimental data set to SVD. The first 10 eigenvalues values and their corresponding RE and IND are summarized in Table 2. The results show that beyond the fourth factor, the consecutive variations tend to zero. Indeed, the SVD analysis suggests a minimum of four factors to explain the systematic variations of the data (or signal) while the rest can be attributed to noise.

Table 2. Singular Values and Their Corresponding RE and IND

factor	eigenvalues value	RE × 10^4	IND × 10^9
1	491.1536	58	22.14
2	42.1777	13	5.07
3	1.8984	6	2.16
4	0.2028	4	1.55
5	0.0742	3	1.25
6	0.0526	3	0.99
7	0.0153	2	0.9
8	0.0106	2	0.83
9	0.007	2	0.78
10	0.0057	2	0.74

Evolving factor analysis (EFA) provides additional information on the principal factors as well as their emergence and disappearance in the process of carbofuran phototransformation. Figure 3 shows three clear emergent profiles, in both forward and backward directions, and a fourth one not well separated from the noise level. The combination of the forward and backward analysis enabled us to estimate the concentration profiles of these factors. These initial estimates of the concentrations are not normalized, where concentration of each species evolves independently from others. These profiles are then subject to resolution by MCR-ALS using soft constraints.

Environmental Science & Technology, Vol 47, No. 15 (August 6, 2013): pg. 8650-8657. DOI.

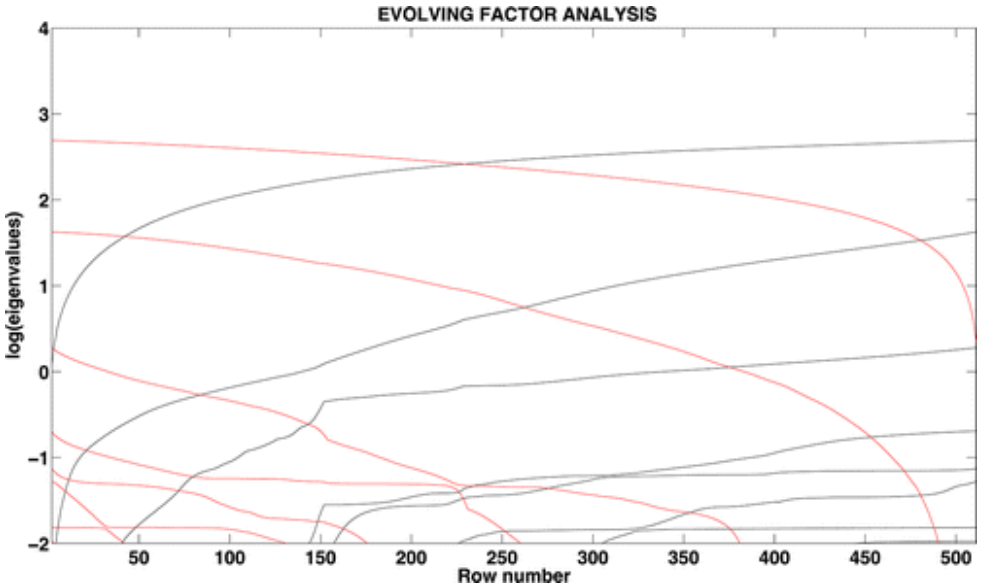

Figure 3. Combined forward and backward EFA.

Resolution with S-MCR-ALS

The first MCR-ALS was performed using the EFA profiles as initial estimates of the concentration profiles and soft-modeling constraints (non-negativity, unimodality, closure) were applied. In fact, the convergence was completed after four iterations with an explained variance of 99.85% and a LOF of 3.262. These values indicate that this resolution fits very well with our experimental data and provide a satisfactory description of the variation with four factors.

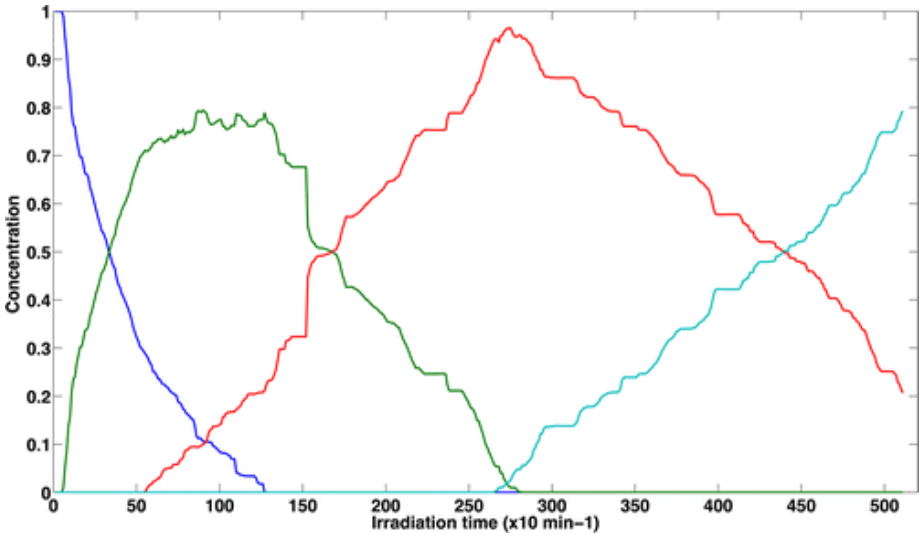

Figure 4. Resolved concentrations by S-MCR-ALS.

Environmental Science & Technology, Vol 47, No. 15 (August 6, 2013): pg. 8650-8657. DOI.

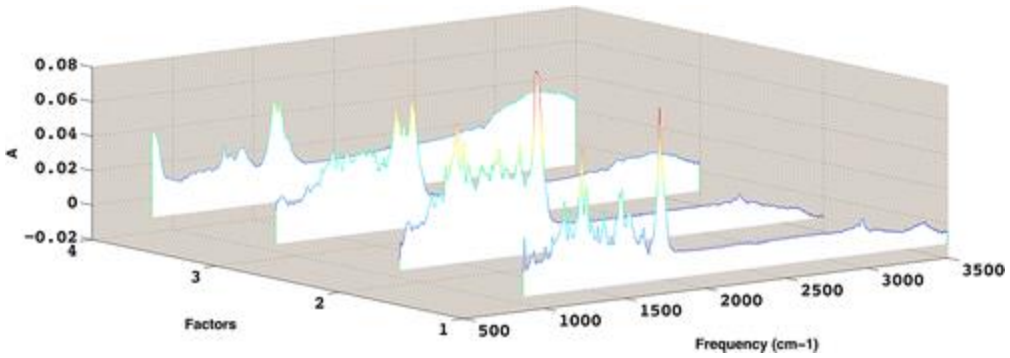

Figure 5. Resolved spectra by S-MCR-ALS.

The concentration profiles obtained by this S-MCR-ALS and their corresponding spectra are shown in Figures 4 and 5. Figure 6 showed that there was good agreement between the calculated and the experimental spectra of carbofuran.

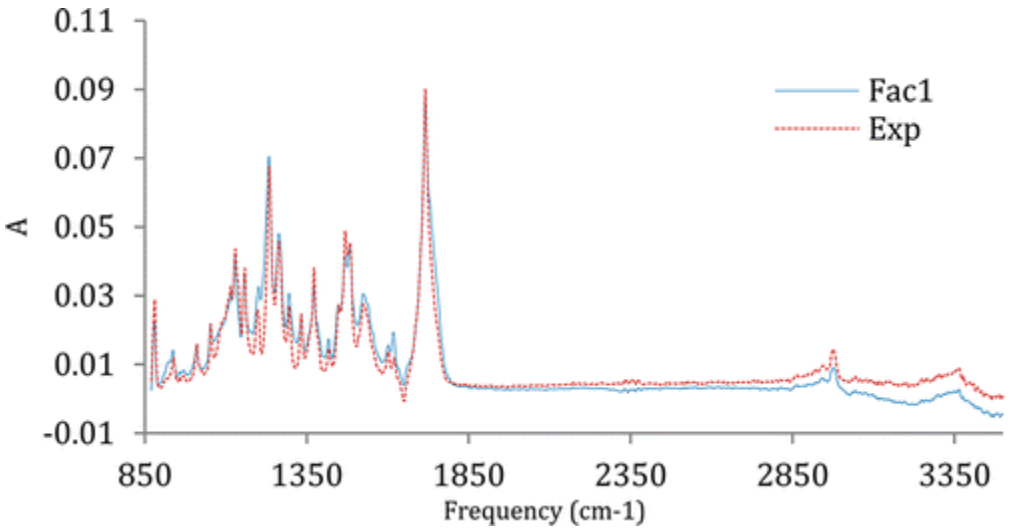

Figure 6. Calculated and experimental spectrum of carbofuran.

Qualitative Analysis

Once the individual spectra were obtained, we were able to carry out a qualitative analysis of the spectra in order to identify the chemical nature of the four factors. For better exposition of the results, the spectra are displayed in a 2D graph (Figure 7). We can summarize the main changes going from one factor to another as a function of irradiation time, as follows:

Environmental Science & Technology, Vol 47, No. 15 (August 6, 2013): pg. 8650-8657. DOI.

The transition from the first factor (carbofuran) to the second factor mainly showed the disappearance of the N–H frequency, decrease of C–N frequency, and growth of an adjacent carbonyl band around 1650 cm^{-1}. Moving from the second to the third factor exhibited an emergence of a large O–H band around 3400 cm^{-1} and a decrease of C–O frequency and C═O frequency. Finally, going from the third to the fourth factor showed an increase in the O–H band, a quasi-disappearance of the C═O band, and an emergence of a new peak around 890 cm^{-1}.

Based on this analysis, the second factor is a product of the cleavage of the C–N carbamate bond, while the third factor is a result of the cleavage of the C–O carbamate group to form a phenol. The fourth factor could be attributed to photoproducts due to further oxidation by hydroxyl radicals.

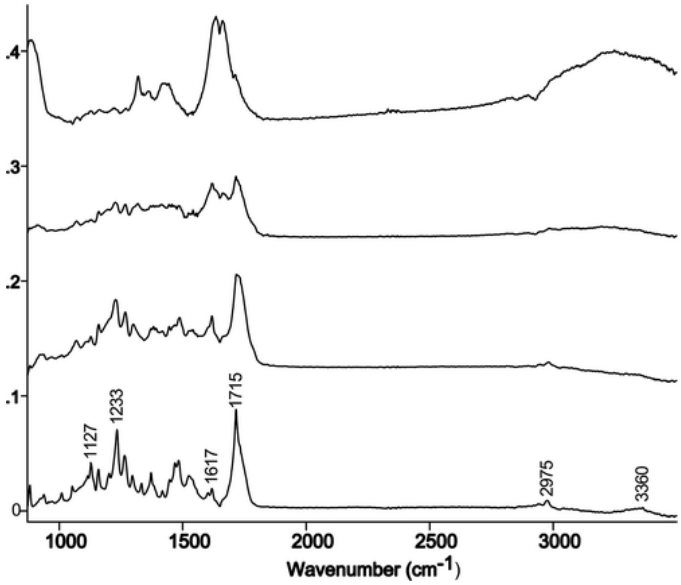

Figure 7. 2D representation of resolved spectra by S-MCR-ALS.

GC-MS

Product identification was also conducted using GC-MS, which was used for qualitative examination of S-MCR-ALS results. GC/MS analysis was obtained after the photolysis and revealed the presence of several compounds. Several elution bands were observed (see the Supporting Information). The first elution band at 22.5 min had a

parent *m*/*z* ratio of 164. This corresponded to Species *3* in Figure 8 (2,3-dihydro-2,2-dimethyl-7-benzofuranol). The second elution band elution band at 30.5 min with an *m*/*z* ratio of 192 was attributed to Species *2*, Figure 8 (2,3-dihydro-2,2-dimethyl-7-benzofuranol-7-formate). Both these species have been reported as intermediates in the Fenton oxidation of carbofuran.[28,36,37] Species *2* was formed by the cleavage of the C–N carbamate bond, while Species *3* was formed by hydrolysis of the formate ester.[37] The third elution band at 32 min was residual carbofuran (Species *1*, Figure 8) with an *m*/*z* ratio of 221.

It is important to mention that this mechanism is in good agreement with the one proposed by Qiquan and Lemley on the carbofuran photodegradation by an $OH^{\bullet}$ hydroxyl radical using the Anodic Fenton Treatment (AFT).[38] According to the authors, the C–N carbamate bond was the primary attack site by the hydroxyl radical, followed by a second attack of the C–O carbamate bond.

Figure 8 shows the proposed structures for the first two major photoproducts with their molecular masses and the main changes observed in the ATR-FTIR spectrum. The cleavage of the C–N carbamate bond resulted in a decrease of N–H and C–N peaks in the infrared spectrum. In addition, the carbonyl band upshifted in factor 2, due to the loss in conjugation with the removal of the amide group. Further photodegradation by cleavage of the phenoxy bond resulted in a decrease of its corresponding infrared peak and the carbonyl peak, while a large O–H band emerged. The band for Species *3* (2,3-dihydro-2,2-dimethyl-7-benzofuranol) at 1670 cm^{-1} was observed in Factor 3.

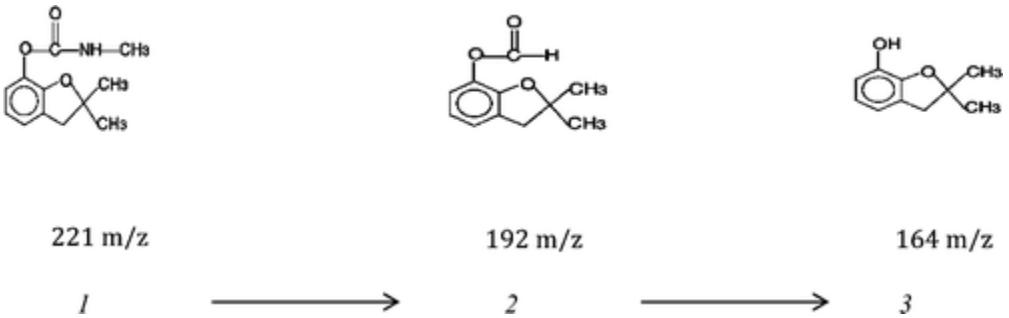

Figure 8. Molecular structures of the major photoproducts and correlated changes in the ATR-FTIR spectrum.

Factor 4 was consistent with the final product in the scheme proposed by Wang and Lemley.[38] In particular, a band was observed at 1670 cm^{-1}, which is consistent with the literature spectrum of Species *4* (7-hydroxy-2,2-dimethyl-3(2H)-benzofuranone). In addition, a broad band at 3400 cm^{-1} was observed in Factor 4 and Species *4*, though this band overlaps with other species present in the final spectrum. Evidence of this species was also found in the GC/MS with a signal at *m/z* = 178, though the band was not well separated from Species *2* (second elution band).

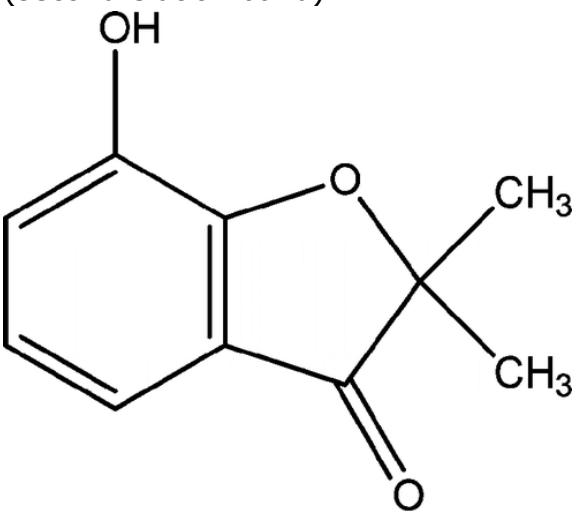

Species *4*

Kinetic Analysis with HS-MCR-ALS

From a practical point of view, it is important not only to detect the formation of photoproducts but also to evaluate their kinetics of formation and degradation. This information can be obtained via a hard modeling by applying a kinetic model as a restriction on the concentration profiles obtained by S-MCR-ALS. The application of this hybrid approach HS-MCR-ALS can therefore enable to describe the reaction mechanism and then to evaluate the rates constants.
From the shape of the concentration profiles resolved by S-MCR-ALS, and taking into account the qualitative analysis, the suggested kinetic model is based on three consecutive reactions where the kinetics of the first two reactions are first-order while the third is zero-order

Environmental Science & Technology, Vol 47, No. 15 (August 6, 2013): pg. 8650-8657. DOI.

$$A \xrightarrow{k_1} B \xrightarrow{k_2} C \xrightarrow{k_3} D$$

where k_1, k_2, and k_3 are the rate constants.

Under our experimental conditions, the continuous irradiation of TiO_2 provides a constant concentration (steady state conditions) of the hydroxyl radicals. Thus, the kinetic laws can be written as

$$\frac{d[A]}{at} = -k_1[A]; \quad \frac{d[B]}{at} = k_1[A] - k_2[B]; \quad \frac{d[C]}{at} = k_2[B] - k_3; \quad \frac{d[D]}{at} = k_3$$

As required for the resolution of this system, the initial concentration of carbofuran (factor 1) has been normalized so that those of other products are zero:

$$A(0) = 1; \quad B(0) = C(0) = D(0) = 0$$

The analytical solution is

$$A(t) = e^{-k_1 t}; \quad B(t) = -\frac{(k_2 - k_1)k_1 e^{-k_1 t}}{(k_1 - k_2)^2} - \frac{k_1 e^{-k_1 t}}{k_1 - k_2}$$

$$C(t) = -\frac{k_2\left[-\frac{1}{e^{k_2 t}} + \frac{k_1^2}{(k_1 - k_2)k_2 e^{k_2 t}} - \frac{k_1}{(k_1 - k_2)e^{k_2 t}}\right]}{k_1 - k_2} - k_3 t + 1$$

where the concentration of *D* can be resolved numerically as follows:

$$D(t) = 1 - A(t) - B(t) - C(t)$$

Using the Levenberg–Marquardt algorithm, first estimations of rate constants are generated by fitting the soft resolved concentrations to simulated ones where the average correlation was 86.9% (H-MCR-ALS). Then these rate constants were used as input for a second S-MCR-ALS, and new resolved concentrations are obtained. Figure 9 illustrates the good agreements between the simulated and the new resolved concentrations, with a better correlation of 96.44%.

Environmental Science & Technology, Vol 47, No. 15 (August 6, 2013): pg. 8650-8657. DOI.

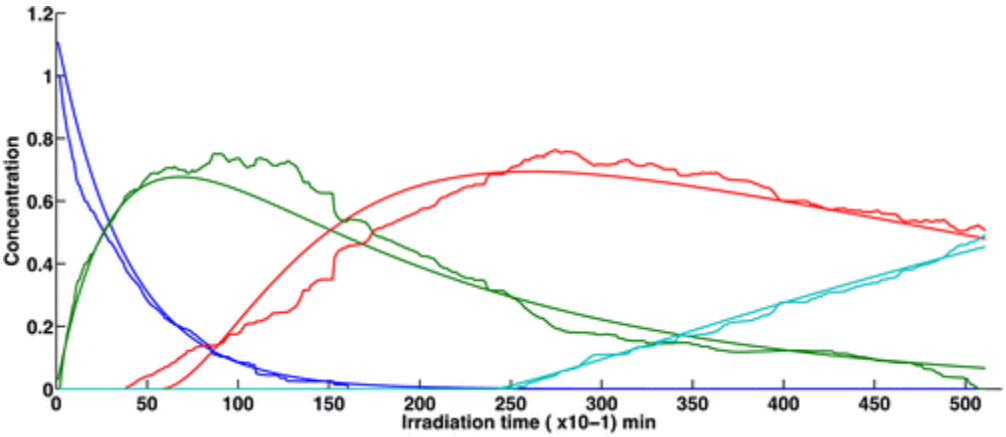

Figure 9. Simulated and resolved concentrations by HS-MCR-ALS.

The HS-MCR-ALS convergence was completed after only three iterations and with an explained variance of 99.87% and LOF of 3.01. These values are better than those obtained previously by S-MCR-ALS. The magnitude of these indicators is also well elucidated by the quality of the spectra recovered by the HS-MCR-ALS procedure (see the Supporting Information).

Table 3 summarizes the updated rates constants, where the average rate constant of carbofuran photodegradation under our experimental conditions was 2.9×10^{-3} min^{-1}, corresponding to a half-life of 4 h. Longer half-lives, ranging from 34 to 170 h, were reported recently in the work of Wang et al., on the effect of TiO_2 on carbofuran photodegradation in soil surface. These times, though, were for the total mineralization of the pesticides, which was not measured in this study (and would be considerably longer than the rates observed here).[39] As introduced earlier, in addition to other factors (chemical composition of the substrate, irradiation source, etc.), the layer thickness would have a substantial effect on the rate of the photodegradation due to heterogeneous conditions within the layer and diffusion process. The zero-order reaction for the last step probably indicates that the photolysis was the rate limiting step.

Table 3. Rate Constants after HS-MCR-ALS Resolution

		rate constants ($\times 10^{-3}$ min^{-1})		
model	**correlation (*R*%)**	k_1	k_2	k_3
A(*t*)	99.45	2.54	-	-
B(*t*)	95.54	3.19	0.55	-
C(*t*)	94.32	3.00	1.05	0.09278

Environmental Science & Technology, Vol 47, No. 15 (August 6, 2013): pg. 8650-8657. DOI.

		rate constants ($\times 10^{-3}$ min^{-1})		
model	**correlation (*R*%)**	k_1	k_2	k_3
av	96.44	2.91	0.80	0.09278

An efficient approach to study in situ photodegradation of pesticides in solid phase has been presented in the present work. As a green alternative to standard chromatographic methods, the ATR-FTIR technique coupled to MCR-ALS methods presents a suitable approach to circumvent difficulties in studying photolysis on solid particles. This approach allowed examining both kinetic and mechanistic aspects of the photochemical reaction in real time. Other competitive chemometric techniques for the analysis of reaction kinetics such as two-dimensional correlation spectroscopy[40] and modulation spectroscopy[41] have been mostly applied to spectral changes due to environmental or conformation changes rather than irreversible reaction schemes.[42] Finally, this investigation will serve as a platform for future works expanded to more complex systems.

Supporting Information

Correlations between the experimental and theoretical frequencies of carbofuran (as calculated by DFT). The evolution of the FTIR spectra during irradiation as 2-D plots for various irradiation times is shown. In addition, the variation as a function of time of the IR bands for various functional groups has been plotted. Graphical plots for the evolving factors analysis are shown as well as the concentrations calculated by S-MCR-ALS and H-MCR-ALS. Selected mass spectra obtained at different elution times during the gas chromatographic elution are shown. This material is available free of charge via the Internet at http://pubs.acs.org.

The authors declare no competing financial interest.

Acknowledgment

We would like to thank the Dr. Hossenlopp group (Chemistry Department, Marquette University) for its technical help. The authors are also grateful to FULBRIGHT & MACECE Organizations for their financial support.

References

[1]Tannock, J.; Wessels, C. L.Determination of carbofuran residues and metabolites in plant material *Pestic. Sci.* 1981, 12, 228– 234

[2]Leppert, B. C.; Markle, J. C.; Helt, R. C.; Fujie, G. H.Determination of carbosulfan and carbofuran residues in plants, soil, and water by gas chromatography *J. Agric. Food Chem.* 1983, 31, 220– 223

[3]Kesselman-Truttmann, J. M.; Hug, S. J.Photodegradation of 4,4′-bis(2-sulfostyryl)biphenyl (DSBP) on metal oxides followed by in situ ATR-FTIR spectroscopy *Environ. Sci. Technol.* 1999, 33, 3171– 3176

[4]Balmer, M. E.; Goss, K. U.; Schwarzenbach, R. P.Photolytic transformation of organic pollutants on soil surfaces-an experimental approach *Environ. Sci. Technol.* 2000, 34, 1240– 1245

[5]Martin, S. T.; Kesselman, J. M.; Park, D. S.; Lewis, N. S.; Hoffmann, M. R.Surface structures of 4-chlorocatechol adsorbed on titanium dioxide *Environ. Sci. Technol.* 1996, 30, 2535– 2542

[6]Biber, M. V.; Stumm, W.An in-situ ATR-FTIR study: the surface coordination of salicylic acid on aluminum and iron(III) oxides *Environ. Sci. Technol.* 1994, 28, 763– 768

[7]Hug, S. J.; Sulzberger, B.In situ Fourier transform infrared spectroscopic evidence for the formation of several different surface complexes of oxalate on TiO_2 in the aqueous phase *Langmuir* 1994, 10, 3587– 3597

[8]Persson, P.; Laiti, E.; Ohman, L. O.Vibration spectroscopy study with phenylphosphonate at the water-aluminum (hydr)oxide interface *J. Colloid Interface Sci.* 1997, 190, 341– 349

[9]Araña, J.; Tello, R.; Dona, R.; Herrera, M.; Gonzalez, D.; Perez, P.High concentrated phenol and 1,2-propylene glycol water solutions treatment by photocatalysis. Catalyst recovery and re-use *Appl. Catal., B* 2001, 30, 1– 10

[10]Araña, J.; Tello, R.; Dona, R.; Herrera, M.; Gonzalez, D.; Perez, P.Highly concentrated phenolic wastewater treatment by the Photo-Fenton reaction, mechanism study by FTIR-ATR *Chemosphere* 2001, 44, 1017– 1023

[11]Hoffmann, M. R.; Martin, S. T.; Choi, W.; Bahnemann, D. W.Environmental applications of semiconductor photocatalysis *Chem. Rev.* 1995, 95, 69– 96

[12]Fenoll, J.; Hellin, P.; Flores, P.; Martinez, C. M.; Navarro, S.Degradation intermediates and reaction pathway of carbofuran in leaching water using TiO_2 and ZnO as photocatalyst under natural sunlight *J. Photochem. Photobiol., A* 2013, 251, 33– 40

[13]Yu, B.; Zeng, J.; Gong, L.; Zhang, M.; Zhang, L.; Chen, X.Investigation of the photocatalytic degradation of organochlorine pesticides on a nano-TiO_2 coated film *Talanta* 2007, 72, 1667– 1674

[14]Fenoll, J.; Hellín, P.; Flores, P.; Martínez, C. M.; Navarro, S.Degradation intermediates and reaction pathway of carbofuran in leaching water using TiO_2 and ZnO as photocatalyst under natural light *J. Photochem. Photobiol., A* 2013, 251, 33– 40

[15]Mahalakshmi, M.; Arabindoo, B.; Palanichamy, M.; Murugesan, V. Photocatalytic degradation of carbofuran using semiconductor oxides *J. Hazard. Mater.* 2007, 143, 240– 245

[16]Menager, M.; Sararkha, M.Simulated solar light phototransformation of organophosphorus azinphos methyl at the surface of clays and goethite *Environ. Sci. Technol.* 2013, 47, 765– 772

[17]McQuillan, A. J.Probing solid-solution interfacial chemistry with ATR-IR spectroscopy of particle films *Adv. Mater*. 2001, 13, 1034– 1038

[18]Almeida, A. R.; Berger, R.; Moulijn, J. A.; Mul, G.Photo-catalytic oxidation of cyclohexane over TiO_2: A novel interpretation of temperature dependent performance *Phys. Chem. Chem. Phys*. 2011, 13, 1345– 1355

[19]Carneiro, C.; Moulijn, J. A.; Mul, G.Photocatalytic oxidation of cyclohexane by titanium dioxide: Catalyst deactivation and regeneration *J. Catal.* 2010, 273, 199– 210

[20]Carneiro, J. T.; Almeida, A. R.; Moulijn, J. A.; Mul, G.Cyclohexane selective photocatalytic oxidation by anatase TiO_2: influence of particle size and crystallinity *Phys. Chem. Chem. Phys.* 2010, 12, 2744– 2750

[21]Dolamic, I.; Bürgi, T.Photocatalysis of dicarboxylic acids over TiO_2: An in situ ATR-IR study *J. Catal.* 2007, 248, 268– 276

[22]Dolamic, I.; Bürgi, T.Photoassisted decomposition of malonic acid on TiO_2 studied by in situ attenuated total reflection infrared spectroscopy *J. Phys. Chem. B* 2006, 110, 14898– 14904

[23]Sivasankar, N.; Weare, W. W.; Frei, H.Direct observation of a hydroperoxide surface intermediate upon visible light-driven water oxidation at an Ir oxide nanocluster catalyst by rapid-scan FT-IR spectroscopy *J. Am. Chem. Soc*. 2011, 133, 12976– 12979

[24]Abbas, O.; Rebufa, C.; Dupuy, N.; Kister, J.FTIR-multivariate curve resolution monitoring of photo-Fenton degradation of phenolic aqueous solutions *Talanta* 2008, 77, 200– 209

[25]Shamsipur, M.; Hemmateenejad, B.; Akhond, M.; Javidnia, K.; Miri, R.A study of the photo-degradation kinetics of nifedipine by multivariate curve resolution analysis *J. Pharm. Biomed. Anal.* 2003, 31, 1013– 1019

[26]Fernandez, C.; de Juan, A.; Callao, M. P.; Larrechi, M. S.Evaluation of the adsorption and rate constants of a photocatalytic degradation by means of HS-MCR-ALS. Study of process variables using experimental design *Chemom. Intell. Lab. Syst.* 2012, 114, 64– 71

Environmental Science & Technology, Vol 47, No. 15 (August 6, 2013): pg. 8650-8657. DOI.

[27]Hemmateenejad, B.; Javidnia, K.; Saeidi-Boroujeni, M.Spectrophotometric monitoring of nimesulide photodegradation by a combined hard-soft multivariate curve resolution-alternative least square method *J. Pharm. Biomed. Anal.* 2008, 47, 625– 630

[28]Atifi, A.; Talipov, M.; Mountacer, H.; Ryan, M. D.; Sarakha, M.A density functional theory and laser flash photolysis investigation of carbofuran photodegradation in aqueous medium *J. Photochem. Photobiol., A* 2012, 235, 1– 6

[29]Frisch, M. J.; Trucks, G. W.; Schlegel, H. B.; Scuseria, G. E.; Robb, M. A.; Cheeseman, J. R.; Scalmani, G.; Barone, B.; Mennucci, B.; Petersson, G. A.; Natatsuji, H.; Caricota, M.; Li, X.; Hratchian, H. P.; Izmaylov, A. F.; Bloino, J.; Zheng, G.; Sonnenberg, J. L.; Hada, M.; Toyota, K.; Fukuda, R.; Hasegawa, J.; Ishida, M.; Nakajima, T.; Honda, Y.; Kitao, O.; Nakai, H.; Vreven, T.; Montgomery, J. A., Jr.; Peralta, J. E.; Ogliaro, F.; Bearpark, M.; Heyd, J. J.; Brothers, E.; Kudin, K. N.; Staroverov, V. N.; Kobayashi, R.; Normand, J.; Raghavachari, K.; Rendell, A.; Burant, J. C.; Iyengar, S. S.; Tomasi, J.; Cossi, M.; Rega, N.; Millam, N. J.; Klene, M.; Knox, J. E.; Cross, J. B.; Bakken, V.; Adamo, C.; Jaramillo, J.; Gomperts, R.; Stratmann, R. E.; Yazyev, O.; Austin, A. J.; Cammi, R.; Pomelli, C.; Ochterski, J. W.; Martin, R. L.; Morokuma, K.; Zakrzewski, V. G.; Voth, G. A.; Salvador, P.; Dannenberg, J. J.; Dapprich, S.; Daniels, A. D.; Farkas, Ö.; Foresman, J. B.; Ortiz, J. V.; Cioslowski, J.; Fox, D. J. *Gaussian 09, Revision B.01*; Gaussian, Inc.: Wallingford, CT, 2009.

[30]Malinowski, E. R. *Factor Analysis in Chemistry*, 2 ed.; John Wiley & Sons, Inc.: New York, 1991.

[31]Malinowski, E. R.Determination of the number of factors and the experimental error in a data matrix *Anal. Chem*. 1977, 49, 612– 617

[32]Gampp, H.; Maeder, M.; Meyer, C. J.; Zuberbühler, A. D.Evolving factor analysis of spectrophotometric titrations: Forget about the law of mass action? *Chimia* 1985, 39, 315– 317

[33]Esteves da Silva, J. C. G.; Tauler, R.Multivariate curve resolution of synchronous fluorescence spectra matrices of fulvic acids obtained as a function of pH *Appl. Spectrosc*. 2006, 60, 1315– 1321

[34]de Juan, A.; Tauler, R.Multivariate curve resolution (MCR) from 2000: progress in concepts and applications *Crit. Rev. Anal. Chem.* 2006, 36, 163– 176

[35]Bevington, P. R. *Data reduction and error analysis in the physical sciences*; McGraw-Hill: New York, 1969.

[36]Bachman, J.; Patterson, H. H.Photodecomposition of the carbamate pesticide carbofuran: Kinetics and the influence of dissolved organic matter *Environ. Sci. Technol.* 1999, 33, 874– 881

[37]Wang, Q.; Lemley, A. T.Competitive degradation and detoxification of carbamate insecticides by membrane anodic Fenton treatment *J. Agric. Food Chem.* 2003, 51, 5382– 5390

[38]Wang, Q.; Lemley, A. T.Oxidative degradation and detoxification of aqueous carbofuran by membrane anodic Fenton treatment *J. Hazard. Mater.* 2003, B98, 241– 255

[39]Wang, D.; Wang, J.; Mu, K.Effect of TiO_2 on photodegradation of several pesticides in surface soil *Huanjing Wuran Yu Fangzhi* 2010, 32, 10– 13

[40]Noda, I.Close-up view on the inner workings of two-dimensional correlation spectroscopy *Vib. Spectrosc*. 2012, 60, 146– 153

[41]Baurecht, D.; Porth, I.; Fringeli, U. P.A new method of phase sensitive detection in modulation spectroscopy applied to temperature induced folding and unfolding of RNase A *Vib. Spectrosc.* 2002, 30, 85– 92

[42]Czarnik-Matusewicz, B.; Pilorz, S.; Zhang, L. P.; Wu, Y.Structure of hexafluoroisopropanol-water mixture studied by FTIR-ATR spectra and selected chemometric methods *J. Mol. Struct.* 2008, 883–884, 195–202

Environmental Science & Technology, Vol 47, No. 15 (August 6, 2013): pg. 8650-8657. DOI.